TEAM Problem 21 Family (V.2009)

(Approved by the International Compumag Society Board at Compumag-2009, Florianópolis, Brazil)

Zhiguang CHENG[1], Norio TAKAHASHI[2], and Behzad FORGHANI[3]
E-mails: [1] emlab@btw.cn, [2]norio@elec.okayama-u.ac.jp, [3]forghani@infolytica.com

Problem 21 Family with 5 sets of engineering-oriented 3-D stray-field loss models is well established. The typical measured and calculated results of these benchmark models have been presented worldwide. This report outlines the new developments of Problem 21 since its update in Version 2005, such as the extensions to model saturation effects, the detailed observation of the electromagnetic field behavior inside the magnetic steel, the variation of iron loss and flux density with different excitation patterns, the addition of two new member-models, and all the updated benchmark results. The above extensions are due to comments and advices received from colleagues on Problem 21 at the CEM-based conferences and are expected to be helpful for further international benchmarking activities and industrial application.

***Index Terms*: Extended benchmark family, nonlinear/hysteresis eddy current problem, stray-field loss, additional iron loss, magnetic flux, solid magnetic steel, silicon steel lamination, shielding, anisotropy modeling, saturation effect, 3-D excitation.**

I. INTRODUCTION

TEAM PROBLEM 21 was proposed at TEAM Workshop-Miami, in 1993[1] and has been updated at TEAM Workshop-Sapporo, in 1999[2] and Compumag-Shenyang, in 2005[3]-[4]. The purpose of all the engineering-oriented upgrades and the Problem 21-based benchmarking activities is to test electromagnetic analysis methods, determine the validity and limitations of both the methods and the software to be used, investigate how to build correct computation models, observe the electromagnetic field behavior of key product-based constructions in detail, and demonstrate the ability to solve practical problems [5]-[15].

At the same time, it is of growing importance to perform such engineering-oriented benchmarking, especially for the design and manufacture of today's extra large electromagnetic devices, such as the extra HV power transformers.

This new version of Problem 21, approved by the ICS Board at Compumag-2009, Florianópolis, Brazil, covers all the new developments of Problem 21 Family taken place since the version in 2005[5],[8]-[13]. The new extensions of Problem 21 are as follows:

1) Increase the exciting source current from the rated 10A up to 50A (50Hz, rms) in order to simulate the possible saturation effects of magnetic steel;

2) Change the excitation pattern to examine the effects on iron loss and flux density;

3) Simplify the magnetic shielding model P21^c-M1 by removing the 10 mm thick magnetic steel plate for further detailed examination of iron loss and flux density inside the laminated sheets. This new member model is called P21^d-M;

4) Other two new member models with hybrid steel welded components that entered into the benchmark family. They are called P21^c-MNM and P21^c-NMN.

Note that all the material property data used in version 2005 and the configuration design of the member models have remained the same in the extended Problem 21 Family.

II. NEW BENCHMARK MODELS

To investigate the multi-steel hybrid structure composed of the magnetic and non-magnetic steel plates, appearing in large power transformer oil-tank walls to reduce iron loss, two verification models, referred to as Problem 21^b-MNM/NMN, have been built[5],[11], as shown in Fig.1. Here 'M' and 'N' denote the magnetic and non-magnetic steel plate respectively.

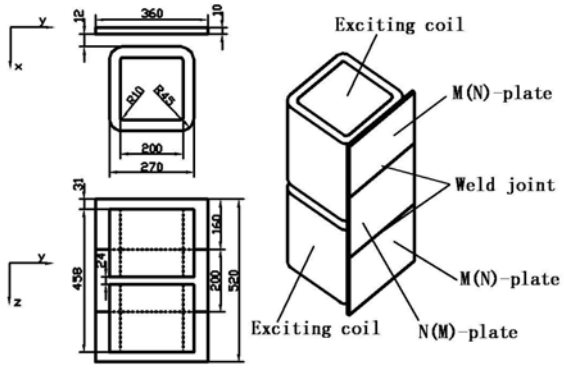

(a) Design of P21^b-MNM/NMN

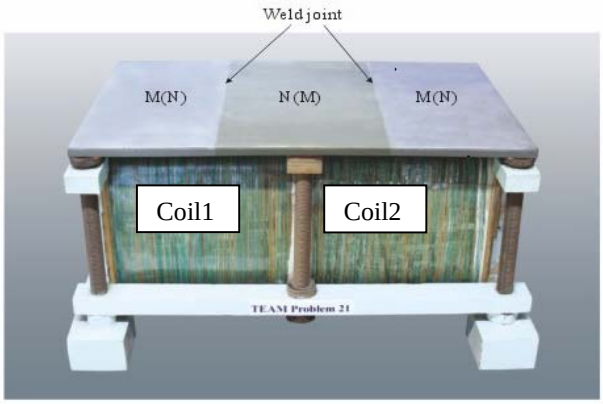

(b) Model P21^b-MNM/NMN(photo)

Fig.1. P21^b-MNM/NMN.

To examine the iron loss and the flux density inside the laminated silicon steel sheets in detail, a simplified model of P21[c]-M1 is proposed where the magnetic plate of 10 mm thick in the original shielding model is removed. This model is called P21[d]-M and is shown in Fig.2.

In the new proposal, the laminated grain-oriented silicon steel sheets (30RGH120) are excited by a perpendicularly applied field in which case the supplementary iron loss concentrated in the surface sheet must be considered[11]-[13].

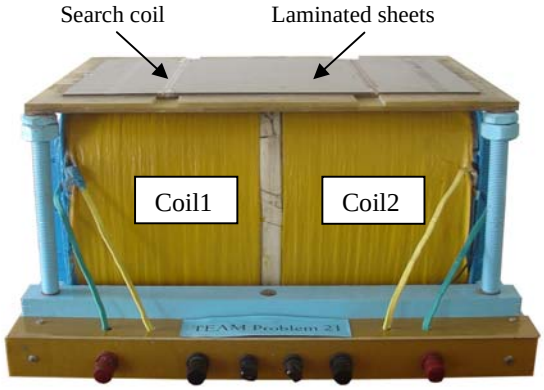

Fig.2. Model P21[d]-M.

The extended Problem 21 Family, including 16 benchmark models, is shown in Table I.

TABLE I
PROBLEM 21 FAMILY (2009)

Member	Models	Problem features	Proposed at
P21	P21-A P21-B	3-D nonlinear eddy current and hysteresis model with multiply connected regions.	TEAM-Miami, USA, 1993[1].
P21[a]	P21[a]-0 P21[a]-1 P21[a]-2 P21[a]-3	3-D linear eddy current model with multiply connected regions.	TEAM-Yichang, China, 1996[14].
P21[b]	P21[b]-MN P21[b]-2M P21[b]-2N	3-D nonlinear eddy current and hysteresis model with magnetic or/and non-magnetic steel plates separately placed.	IEE CEM, Bournemouth, UK, 2002[15].
	P21[b]-MNM P21[b]-NMN	3-D nonlinear eddy current and hysteresis model with magnetic and non-magnetic steel plates welded together.	ACES, Miami, USA, 2006[5].
P21[c]	P21[c]-M1 P21[c]-M2 P21[c]-EM1 P21[c]-EM2	Magnetic shielding and electromagnetic shielding models: 3-D nonlinear eddy current and hysteresis model with anisotropic lamination.	Compumag-Shenyang, China, 2005[4].
P21[d]	P21[d]-M	3-D nonlinear eddy current and hysteresis model with anisotropic lamination without solid magnetic steel.	IEEE CEFC-Athens, Greece, 2008[11],[13].

Note that the configuration of the models, the input and output data, the measured and calculated results of the former member-models of Problem 21 Family[5],[14],[15]-[38], and the property data of the magnetic steel material used in Problem 21 Family can be found in Appendix 1 to Appendix 4, respectively.

III. EXTENDED BENCHMARKING RESULTS

A. *Increasing the Exciting Current*

In order to model the saturated magnetic steel, the B-H curve given in the definition of Model B of the Problem 21 (P21-B) should be extrapolated when the B_{max} inside the magnetic steel plate goes over the maximum value of flux density (B) of the B-H curve during the iteration process. The extrapolated part of the B-H curve of the magnetic steel (A3) used in P21-B is expressed as

$$B = \mu_0 H - 1.9538 \times 10^{-10} H^2 + 1.9043 \times 10^{-5} H + 1.5729 \quad (1.85\text{T} < B < 2.1\text{T})$$

$$B = \mu_0 H + 2.0368 \quad (B > 2.1\text{T})$$

For the same reason as stated above, the magnetic property curves of the grain-oriented silicon steel sheet 30RGH120 should be extrapolated in an adequate way when the exciting current exceeds beyond a certain point.

The measured and calculated results of both iron loss and flux inside the magnetic steel plate of P21-B with different exciting currents, ranging from 5A to 50A, are shown in Table II and Table III respectively, and they are practically in good agreement.

TABLE II
MEASURED AND CALCULATED RESULTS OF IRON LOSS (P21-B)

Exciting currents (A,rms,50Hz)	Meas. P_{meas} . (W)	Calc.(by $\boldsymbol{A}_r$-V-$\boldsymbol{A}_r$) $P_{calc.}$(W)	$(P_{calc.}- P_{meas.})/P_{meas.}$ (%)
5	3.30	3.30	0.0
10	11.97	12.04	0.6
15	26.89	27.12	0.9
20	49.59	50.92	2.7
25	82.39	84.78	2.9
30	123.70	128.67	4.0
35	179.10	183.15	2.3
40	248.00	250.45	1.0
45	330.00	330.91	0.3
50	423.00	425.07	0.5

TABLE III
MEASURED AND CALCULATED RESULTS OF FLUX INSIDE MAGNETIC STEEL (P21-B)

Exciting currents (A,rms,50Hz)	Meas. $\Phi_{meas.}$(mWb)	Calc.(by $\boldsymbol{A}_r$-V-$\boldsymbol{A}_r$) $\Phi_{calc.}$ (mWb)	$(\Phi_{calc.}- \Phi_{meas.})/\Phi_{meas.}$ (%)
5	0.158	0.151	-4.12
10	0.318	0.306	-3.86
15	0.478	0.458	-4.13
20	0.618	0.605	-1.98
25	0.770	0.750	-2.66
30	0.936	0.890	-4.90
35	1.064	1.024	-3.76
40	1.206	1.152	-4.48
45	1.357	1.276	-5.97
50	1.486	1.396	-6.06

B. *Magnetic Flux Density inside the Silicon Lamination*

To measure the distribution of flux density inside the laminated sheets of P21^{d}-M, a number of search coils with 20 turns each are placed at different positions, as shown in Fig.3.

It can be seen that the number of the sheets is different inside each search coil. For example, there is only one sheet inside search coils no.1 and no.2, but there are two sheets inside search coils no.3 and no.4. The search coils are made of very thin wire (ϕ0.056mm).

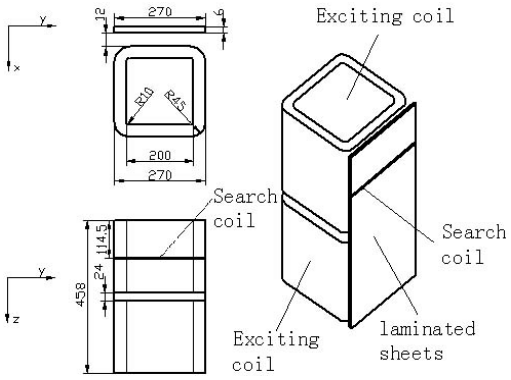

(a) P21-M1

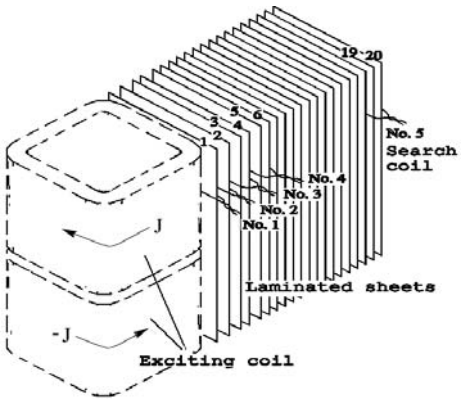

(b) Location of search coil (sketch)

Fig.3. Measurement of flux density inside sheets.

The measured and calculated waveforms of the flux density inside different sheet-layers (form no.1 to no.4) at the exciting current of 25A (rms, 50Hz) are shown in Fig.4, and the related data are also listed in Appendix 2 for reference.

Fig.4 shows that the waveforms of flux density inside the laminated sheets are distorted at different levels and the measured and calculated results agree well.

The measured and calculated magnetic flux density results inside the different sheet-layers at 25A (rms, 50Hz) are listed in Table IV and Table V for reference. The locations of the search coils can be found in Fig.3(b).

C. *Iron Loss and Flux under Different Excitation Patterns*

In Problem 21 Family, the common exciting source is composed of two exciting coils with the same number of turns and the same dimensions, with the exciting currents of the two coils flowing in opposite directions. To further examine the effect of different excitation patterns on iron loss and flux, three test cases based on the exciting currents in coils 1 and 2 (see Fig.2) are proposed[13],[38], as shown in Table VI. Fig.5 shows the 2-D magnetic field distributions for three cases.

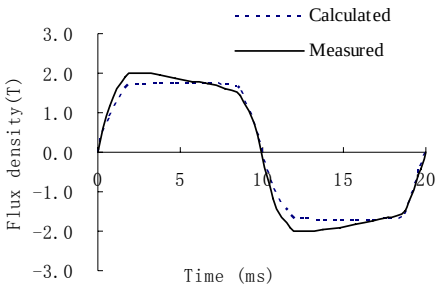

(a) no.1

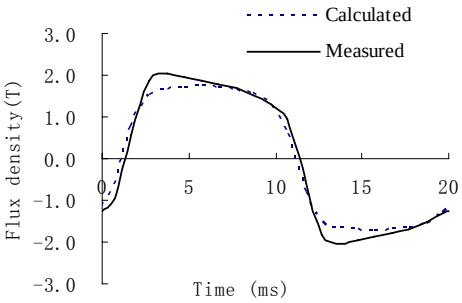

(b) no.2

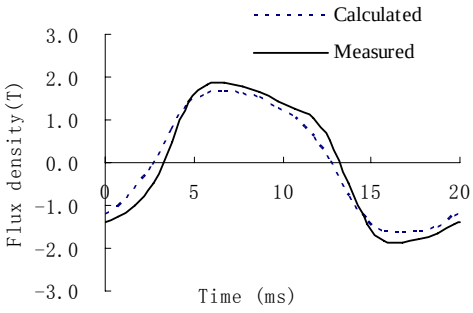

(c) no.3

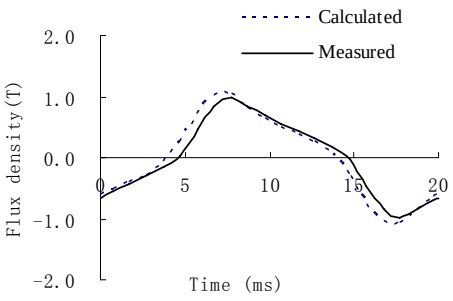

(d) no.4

Fig.4. Waveforms of flux density inside the lamination-layers (exciting current: 25A, rms, 50Hz).

The exciting currents in the coils range from 0A to ±50A (rms, 50Hz). The corresponding analysis (by $\boldsymbol{A_r}$-$\boldsymbol{V}$-$\boldsymbol{A_r}$ solver and/or $\boldsymbol{T}$-$\boldsymbol{\Omega}$ based MagNet, Infolytica) and measurement (using Power Analyzer WT-3000, Yokogawa, Japan) of iron loss and flux of P21-B and P21^{d}-M have been carried out based on the prescribed cases.

TABLE IV
CALCULATED FLUX DENSITY RESULTS OF P21-M1 (LAYERS NO.1～NO.4)

Time(ms)	No.1	No. 2	No.3	No.4
0.0	0.000	-1.110	-1.215	-0.621
0.72	0.921	-0.614	-1.043	-0.533
1.72	1.611	0.769	-0.628	-0.412
2.72	1.695	1.503	-0.058	-0.278
3.72	1.737	1.671	0.777	-0.070
4.72	1.751	1.715	1.386	0.271
5.72	1.742	1.721	1.615	0.716
6.72	1.722	1.706	1.638	1.024
7.72	1.683	1.673	1.609	1.052
8.72	1.557	1.580	1.500	0.804
9.72	0.363	1.306	1.278	0.624
10.72	-0.924	0.609	1.035	0.504
11.72	-1.612	-0.774	0.618	0.386
12.72	-1.695	-1.505	0.046	0.252
13.72	-1.738	-1.671	-0.788	0.045
14.72	-1.751	-1.716	-1.394	-0.298
15.72	-1.742	-1.722	-1.617	-0.744
16.72	-1.723	-1.706	-1.639	-1.050
17.72	-1.683	-1.673	-1.611	-1.078
18.72	-1.558	-1.581	-1.503	-0.830
19.72	-0.366	-1.308	-1.282	-0.650
20.0	0.000	-1.110	-1.214	-0.615

TABLE V
MEASURED FLUX DENSITY RESULTS OF P21-M1 (LAYERS NO.1～NO.4)

Time(ms)	No.1 B1(T)	No. 2 B2(T)	No.3 B3(T)	No.4 B4(T)
0.0	0.014	-1.241	-1.401	-0.654
0.72	1.195	-0.967	-1.268	-0.561
1.72	1.930	0.547	-1.021	-0.433
2.72	2.021	1.856	-0.494	-0.304
3.72	1.976	2.057	0.492	-0.158
4.72	1.889	1.969	1.433	0.039
5.72	1.803	1.877	1.840	0.458
6.72	1.718	1.782	1.874	0.842
7.72	1.628	1.683	1.788	0.981
8.72	1.444	1.522	1.637	0.852
9.72	0.428	1.300	1.456	0.694
10.72	-1.169	0.965	1.273	0.564
11.72	-1.926	-0.519	1.031	0.437
12.72	-2.022	-1.845	0.512	0.309
13.72	-1.973	-2.055	-0.498	0.161
14.72	-1.892	-1.975	-1.438	-0.038
15.72	-1.814	-1.887	-1.843	-0.459
16.72	-1.730	-1.801	-1.872	-0.843
17.72	-1.641	-1.706	-1.787	-0.981
18.72	-1.457	-1.541	-1.636	-0.851
19.72	-0.436	-1.318	-1.455	-0.695
20.0	-0.017	-1.247	-1.405	-0.657

TABLE VI
DIFFERENT EXCITATION CONDITIONS

Cases	Exciting currents (50Hz)		Main property of flux
	In Coil 1	In Coil 2	
I	**J**	**-J**	Perpendicular to steel plate (or lamination)
II	**J**	**J**	Parallel to steel plate (or lamination)
III	**J**	**0**	Partly perpendicular, partly parallel

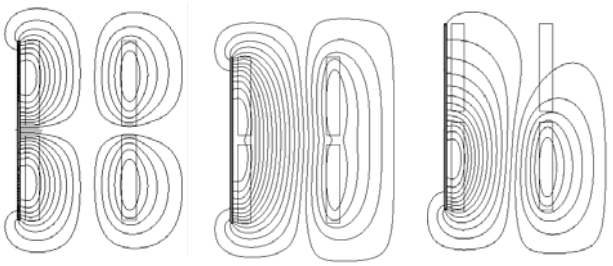

(a) Case I (b) Case II (c) Case III

Fig.5. 2-D magnetic filed distributions.

The available results of iron loss and flux with respect to P21-B are shown in Tables VII~VIII for Case II and Case III[13], while the results for Case I can be found in Tables II and III.

TABLE VII
IRON LOSS INSIDE MAGNETIC STEEL PLATE OF P21-B

Exciting currents (A,rms,50Hz	Case II/*P2*(W) (by $\boldsymbol{T}$-Ω)		Case III/*P3*(W) (by $\boldsymbol{T}$-Ω)	
	Meas.	Calc.	Meas.	Calc.
10	11.61	10.92	6.04	6.57
15	26.52	25.80	13.48	14.43
20	47.16	48.32	24.35	25.49
25	74.40	72.36	39.44	40.12
30	107.60	101.12	58.90	58.64
35	155.00	150.76	83.27	81.32
40	205.00	197.32	114.10	108.72
45	258.00	249.92	146.37	152.92
50	335.50	316.82	189.00	190.42

TABLE VIII
FLUX INSIDE MAGNETIC STEEL PLATE OF P21-B

Exciting currents (A,rms,50Hz	CaseII/ϕ*2*((mWb) (by $\boldsymbol{T}$-Ω)		CaseIII/ϕ*3*((mWb) (by $\boldsymbol{T}$-Ω)	
	Meas.	Calc.	Meas.	Calc.
10	0.341	0.356	0.326	0.318
15	0.513	0.538	0.492	0.481
20	0.679	0.687	0.652	0.637
25	0.834	0.841	0.808	0.780
30	0.983	0.970	0.967	1.003
35	1.129	1.141	1.113	1.108
40	1.270	1.300	1.256	1.260
45	1.404	1.410	1.398	1.413
50	1.540	1.580	1.537	1.500

The results of iron loss and magnetic flux with respect to P21^d-M are shown in Tables IX~X for Case I to Case III.

TABLE IX
IRON LOSS OF LAMINATED SHEETS
(P21^d-M)

Exciting currents (A,rms,50Hz)	Case I/*P1* (W) (by ***T***-Ω)		Case II/*P2*(W) (by ***T***-Ω)		Case III/*P3*(W) (by ***T***-Ω)	
	Meas.	Calc.	Meas.	Calc.	Meas.	Calc.
10	2.20	2.33	0.66	0.62	0.59	0.57
15	5.30	5.04	1.43	1.33	1.39	1.26
20	10.20	10.32	2.71	2.45	2.99	2.76
25	16.80	16.33	4.72	4.49	5.19	4.91

TABLE X
FLUX INSIDE TWENTY SHEETS UNDER EXCITING SOURCE
(P21^d-M)

Exciting currents (A,rms,50Hz)	Case I/ϕ*1* (mWb) (by ***T***-Ω)		Case II/ϕ*2*(mWb) (by ***T***-Ω)		CaseIII/ϕ*3*(mWb) (by ***T***-Ω)	
	Meas.	Calc.	Meas.	Calc.	Meas.	Calc.
10	0.297	0.311	0.357	0.381	0.329	0.323
15	0.444	0.447	0.532	0.569	0.490	0.501
20	0.589	0.594	0.708	0.707	0.652	0.672
25	0.738	0.702	0.886	0.893	0.817	0.832

The results shown in Tables IX ~X can be summarized as follows:

1) The calculated results of iron loss agree well with the measured ones for P21-B and P21^d-M for all the cases and there is agreement for the flux results for P21-B and P21^d-M;

2) The field quantity (such as the iron loss and/or flux) relationships among the three cases are quite different for the solid plate and the laminated sheets under the same applied sources, i.e., a different result is obtained for each excitation pattern.

IV. BENCHMARKING REMARKS

Problem 21 Family is further developed following comments from colleagues and the extended benchmarking results show that:

1) According to the presentations regarding Problem 21 Family, the calculated results of iron loss and magnetic flux at the rated exciting currents of 10A(rms, 50Hz) of all the former member models agree well with the measured ones.

2) The extended Problem 21 Family can now be used to model the saturation effect in the magnetic plate or the lamination by increasing the exciting currents. In particular, the member model P21^d-M allows detailed examination of the electromagnetic behavior inside laminated sheets.

3) The variation of both the iron loss and the magnetic flux with the excitation patterns can be investigated inside the laminated sheets and the magnetic plate.

4) The measured and calculated results obtained until now for the extended Problem 21 Family are practically in agreement.

5) With efficient and practical solvers, it is certainly expected to have improved results which will be helpful in the future benchmarking activities and industrial application.

All the comments and advices from colleagues have been very helpful in developing the new version of Problem 21, which has been approved by the Board of the International Compumag Society. Any new developments or further improvements of the results for this TEAM Problem certainly depend on contributions from researchers around the world.

REFERENCES

[1] Z.Cheng, Q.Hu, S.Gao, Z.Liu, C.Ye, M.Wu, J.Wang and H.Zhu, "An engineering-oriented loss model (Problem 21)," Proc. of the International TEAM Workshop, Miami, pp.137-143, 1993.

[2] Z.Cheng, N.Takahashi, S.Gao and T.Sakura, "Loss analysis based on revised version of TEAM Problem 21," TEAM-Sapporo, 1999.

[3] Z.Cheng, N. Takahashi, S. Yang, T. Asano, Q. Hu, S. Gao, X. Ren, H. Yang, L. Liu, L. Gou, "Loss spectrum and electromagnetic behavior of problem 21 family", *IEEE Trans.on Magn*., vol.42, no.4, pp.1467-1470, 2006.

[4] Z.Cheng, N.Takahashi, S.Yan, T.Asano, Q.Hu and X.Ren, "Proposal of Problem 21-based shielding model (Problem 21$^{'}$)," Proc. of TEAM Workshop, Shenyang, pp.15-20, 2005.

[5] Z.Cheng, N.Takahashi, S.Liu, S.Yang, C.Fan, Qi.Hu, L.Liu, M.Guo, and J.Zhang, "Benchmarking-based approach to engineering stray-field loss problems," presented at ACES-Miami, USA, 2006.

[6] N.Takahashi, T.Sakura and Z.Cheng, "Nonlinear analysis of eddy current and hysteresis losses of 3-D stray field loss model（Problem 21）," *IEEE Trans. on Magn*.,vol.37, no.5, pp.3672-3675, 2001.

[7] Z.Cheng, R.Hao, N.Takahashi, Q.Hu and C.Fan, "Engineering-oriented benchmarking of Problem 21 family and experimental verification," *IEEE Trans. on Magn.*, vol. 40, no.2, pp.1394-1397, 2004.

[8] Z.Cheng, N.Takahashi,S.Yang,C.Fan,M.Guo,L.Liu, J.Zhang and S.Gao, "Eddy current and loss analysis of multi-steel configuration and validation," *IEEE Trans. on Magn.*, vol.43, no.4, pp.1737-1740, 2007.

[9] Z.Cheng, N.Takahashi, B.Forghani, et al, *Electromagnetic and thermal filed modeling and application in electrical engineering*, Science Press, Beijing, 2009.

[10] Z.Cheng, N.Takahashi, B.Forghani, Y.Du,J.Zhang, L.Liu, Y.Fan, Q.Hu,C.Jiao, and J.Wang, " Large power transformer-based stray-field loss modeling and validation," Electric Machines and Drives Conference. IEEE International, pp.548-555 (Digital Object Identifier: 10.1109/IEMDC.2009.5075260), 2009.

[11] Z.Cheng, N.Takahashi, B.Forghani, G.Gilbert, J.Zhang, L.Liu, Y.Fan, X.Zhang, Y.Du, J.Wang, and C.Jiao, "Analysis and measurements of iron loss and flux inside silicon steel laminations," *IEEE Trans. on Magn.*, vol.45, no.3, pp.1222-1225, 2009.

[12] Y. Du, Z. Cheng, B.Forghani, J. Zhang, L. Liu, Y. Fan, W. Wu, Z. Zhai and J. Wang, "Additional iron loss modeling inside silicon steel laminations," Electric Machines and Drives Conference. IEEE International, pp.826-831(Digital Object Identifier: 10.1109/IEMDC. 2009.5075299), 2009

[13] Z.Cheng, N.Takahashi, B.Forghani, G. Gilbert, Y.Du, Y.Fan, L.Liu, Z.Zhai, W.Wu, and J.Zhang, "Effect of excitation patterns on both iron loss and flux in solid and laminated steel configurations," presented at Compumag-Florianópolis, Brazil, 2009.

[14] S.Gao, M.Wu, H.He, J.Wang, Z.Liu, Q.Hu and Z.Cheng, "Problem 21$^+$: slotted non-magnetic steel plate driven by Problem 21's source," Proc. of the ICEF & TEAM Workshop, Yichang, pp.366-370, 1996.

[15] Z.Cheng, N.Takahashi, Q.Hu and C.Fan, "TEAM-based benchmark family: Problem 21/21$^+$/21*," Proc. of the 4th IEE CEM, UK, 2002.

[16] N.Takahashi, K.Fujiwara and J.Takehara, "Basic study on characteristics of magnetic shielding and electromagnetic shielding," Software for Electrical Engineering Analysis and Design V (Edited: Wessex Institute of Technology), WIT Press, pp.79-86, 2001.

[17] O.Biro and K.Preis, "Solution of TEAM benchmark problem 21 (an engineering-oriented loss model)," Proceeding of the International TEAM Workshop, Aix-Les-Bains, pp.25-27, 1994.

[18] Z.Cheng, Q.Hu, S.Gao, Z.Liu, C.Ye and M.Wu, "On the benchmark solution of a typical engineering loss problem," 10th Annual Review of Progress in Applied Computational Electromagnetics, Monterey, pp.335-342, 1994.

[19] Z.Cheng, Q.Hu, S.Gao, Z.Liu, C.Ye and M.Wu, "Supplementary report on problem 21," Proc. of the International TEAM Workshop, Aix-Les-Bains, France, pp.37-47, 1994.
[20] T.Nakata, N.Takahashi, K.Fujiwara, H.Ohashi and H.Zhu, "Analysis of an engineering-oriented loss model(Problem 21)," Proc. of the TEAM Workshop, Seoul, pp.51-55, 1994.
[21] T.Nakata, N.Takahashi, K.Fujiwara, H.Ohashi and H.Zhu, "Analysis of flux and eddy current distribution of 3-D stray-field loss model (Problem 21)," Proc.of the International TEAM Workshop, Aix-Les-Bains, pp.21-24, 1994.
[22] J.P.Bastos, N.Ida, R.C.Mesquita and J.Hector, "Problem 21:solution using edge elements and a vector potential **A**," Proc. of the International TEAM Workshop,Berlin, pp.71-75, 1995.
[23] Z.Cheng, Q.Hu, S.Gao, Z.Liu and M.Wu, "Stray-field loss analysis and measurement (Problem 21)," Proc. of the International TEAM Workshop, Berlin, pp.62-66, 1995.
[24] N.Takahashi, T.Nakata, K.Fujiwara, K.Muramatsu and T.Torii, "Time periodic finite element analysis of Problem 21," Proc. of the International TEAM Workshop, Berlin, pp.56-61, 1995.
[25] J.Gu, W.Yan and Q.Yang, "Computation of flux and eddy current distributions of an engineering-oriented loss model (Problem 21)," Proc. of the International TEAM Workshop, Berlin, pp.52-55, 1995.
[26] L.Li,X.Cui and J.Yuan, "Numerical calculation of 3D eddy current loss and magnetic field (Problem 21)," Proc. of the International TEAM Workshop, Berlin, 67-70, 1995.
[27] O.Biro, K.Pries and K.R.Richter, "Various FEM formulation for the calculation of the calculation of transient 3D eddy currents in nonlinear media," *IEEE Trans. on Magn.*, vol.31, no.3, pp.1307-1312, 1995.
[28] T.Nakata and K.Muramutsu, "Has the 3D magnetic field analysis come into practical application?" (invited), CBMAG, pp.7-12, 1995.
[29] J.Fetzer, S.Kurz, and G.Lehner, "The solution of TEAM workshop Problem 21 using BEM-FEM coupling," Proc. of the International TEAM Workshop, Okayama, pp.19-22, 1996.
[30] C.Golavanov, Y.Marechal and G.Meunir, "Solution of TEAM workshop problem 21," Proc. of the International TEAM Workshop, Okayama, pp.26-30, 1996.
[31] P.J.Leonard, D.Rodger, G..Ciuprina and D.Loan, "Solution of TEAM Problem No.21," Proc. of TEAM Worshop, Graz, pp.17-19, 1996.
[32] Y.Yao, D.Xie and B.Bai, "The application of the modified impedance boundary condition to the Problem 21," Electromagnetic Field Problems and Applications (ed. by Zhou Keding), ICEF, pp.376-379, 1996.
[33] H.Lin, "Solution of TEAM workshop Problem 21 with improved sub-structure technique," Electromagnetic Field Problems and Applications (ed. by Zhou Keding), ICEF, pp.380-382, 1996.
[34] Z.Cheng, S.Gao, J.Wang, H.He, Z.Liu, M.Wu, H.Li and Q.Hu, "Loss evaluation of non-magnetic tie-plates in transformers," COMPEL, vol.17, no.1/2/3, pp.347-351, 1998.
[35] Z.Cheng, S.Gao and L.Li, *Eddy Current Analysis and Validation in Electrical Engineering*, Higher Education Press, Beijing, 2001.
[36] I.Sebestyen and M.Kuczmann, "Investigation of different approaches for iron loss prediction methods using TEAM Problem 21," Record of the 15th Compumag Conference on the Computation of Electromagnetic Fields, Shenyang, 2005, vol.II, pp.268-269; Proc. of TEAM Workshop, Shenyang, pp.5-6, 2005.
[37] A.Sitzia, A.Baker, A.Davies, and L.Clough, "Specialised software tools for transformer analysis," presented at International Colloquium Transformer Research and Asset Management, Cavtat, Croatia, Nov. 12-14, 2009.
[38] Z.Cheng, Q.Hu, N.Takahashi, and B.Forghani, "Stray-field loss modelling in transformers," presented at International Colloquium Transformer Research and Asset Management, Cavtat, Croatia, Nov. 12-14, 2009.

==========

Appendix 1 Configuration of Models

==========

The configuration of the 13 member models of the Problem 21 Family are described below – also see Appendix 6.

A. Principal Member Models of Problem 21

TEAM Problem 21 shown in Fig.A1-1 has two sub-models: Model A and Model B, referred to as principal models. Model A consists of two exciting coils of the same specifications and two magnetic steel plates. In the center of one steel plate, there is a rectangular hole. Model B has the same exciting coils as Model A and only one steel plate without a hole. The exciting currents in the two coils flow in opposite directions.

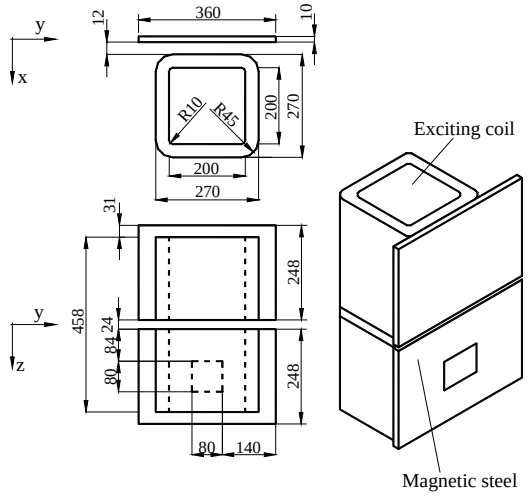

(a) Model A

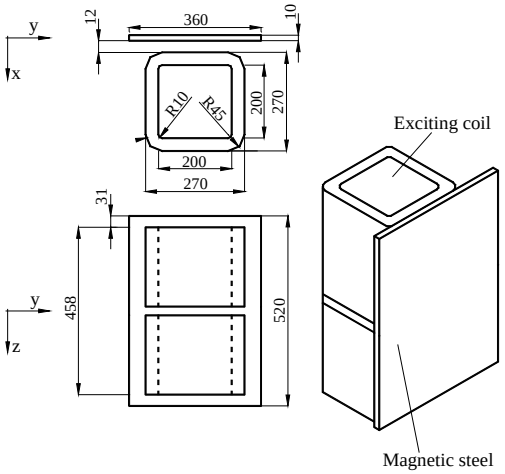

(b) Model B

Fig. A1-1. TEAM Problem 21.

B. Problem 21[a]

Problem 21[a], as a member of the benchmark family, has four sub-models, denoted by P21[a]-0, P21[a]-1, P21[a]-2 and P21[a]-3, where 0~3 indicate the number of slits made in the non-magnetic steel plates. The plates are excited by the same AC source as shown in Fig.A1-2.

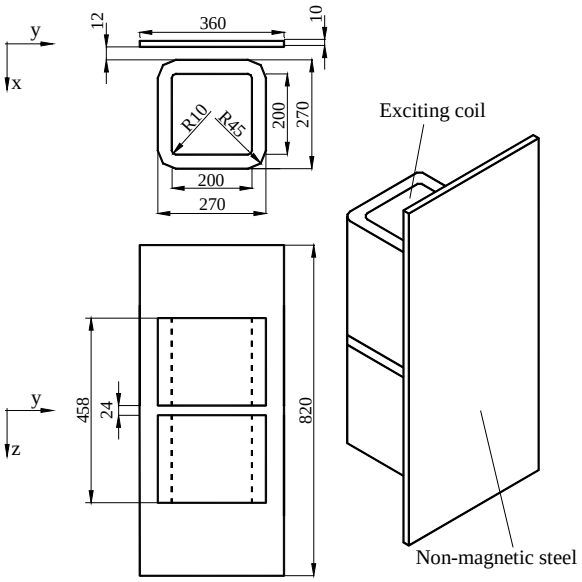

(a)P21[a]-0

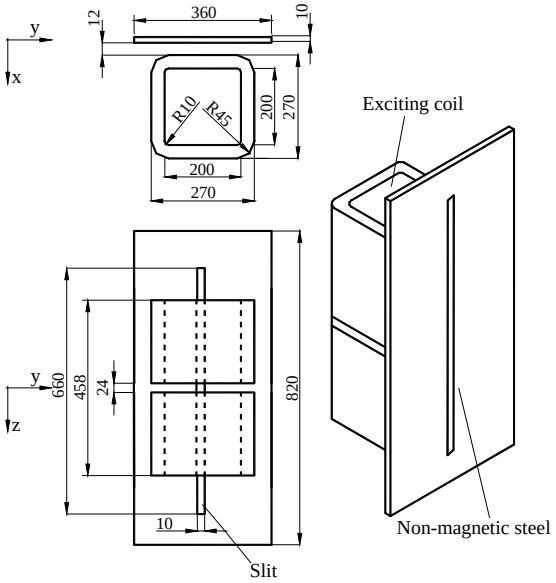

(b) P21[a]-1

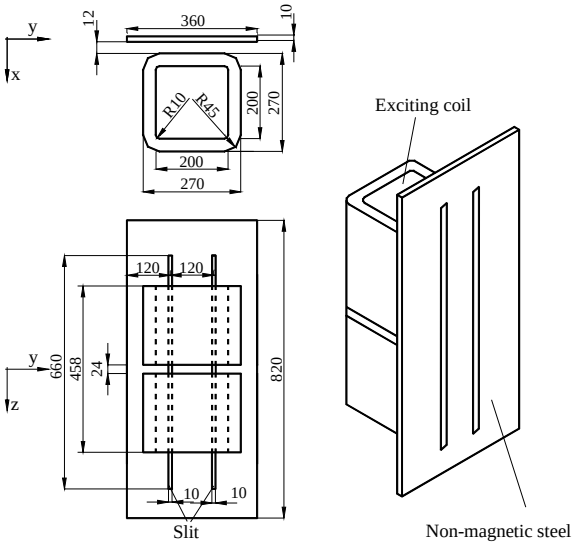

(c) P21[a]-2

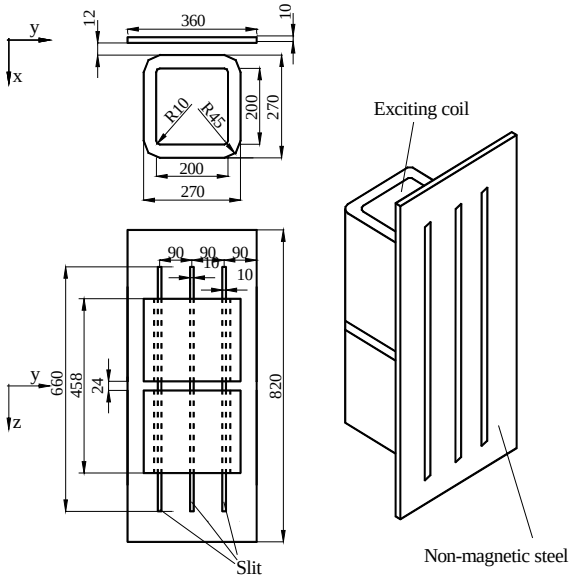

(d) P21[a]-3

Fig. A1-2. Problem 21[a].

Note that the length, width, and depth of each slit made in the non-magnetic steel plate are 660mm, 10mm, and 10mm respectively.

C. Problem 21[b]

Problem 21[b] has three sub-models called P21[b]-MN, P21[b]-2M and P21[b]-2N, where 'M' and 'N' stand for magnetic steel plate and non-magnetic steel plate respectively. Model details are provided in Fig.A1-3. The configurations of the three sub-models are the same.

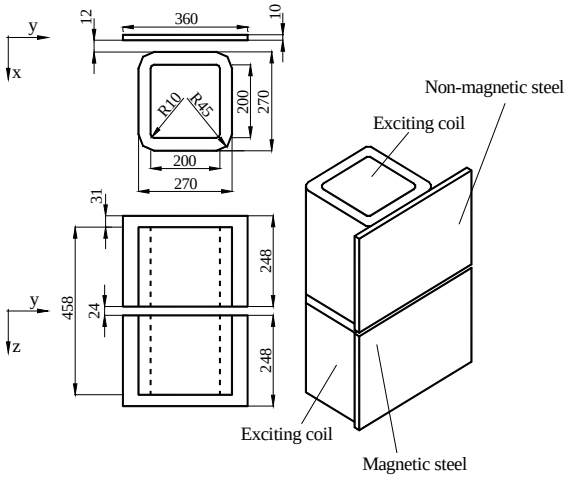

(a) P21[b]-MN

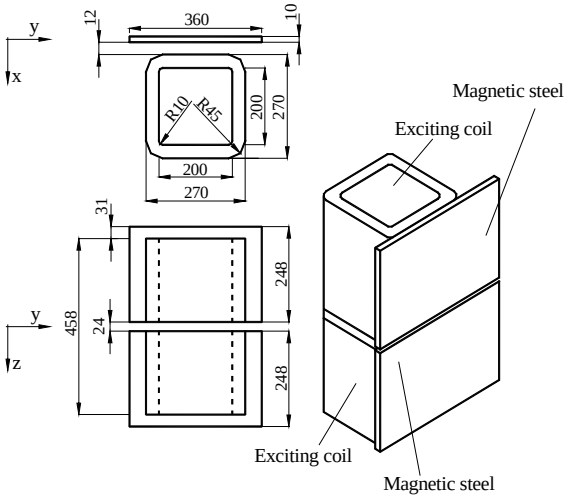

(b) P21[b]-2M

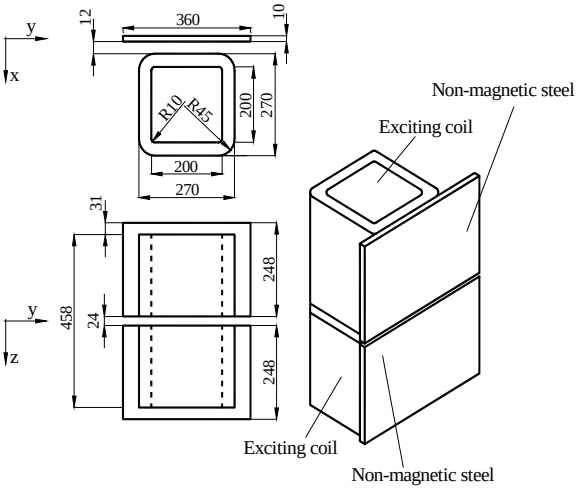

(c) P21[b]-2N

Fig. A1-3. Problem 21[b].

D. Problem 21^c

Problem 21^c includes magnetic (M) and electromagnetic (EM) shields[6], made of anisotropic silicon steel sheets and copper plates respectively. The shields are of two types, either having one single silicon steel sheet or copper plate, referred to as type 1(i.e., M1 or EM1), or three separated silicon steel sheets or plates, referred to as type 2(i.e., M2 or EM2). The dimensions of the corresponding magnetic and electromagnetic shields are shown in Fig.A1-4.

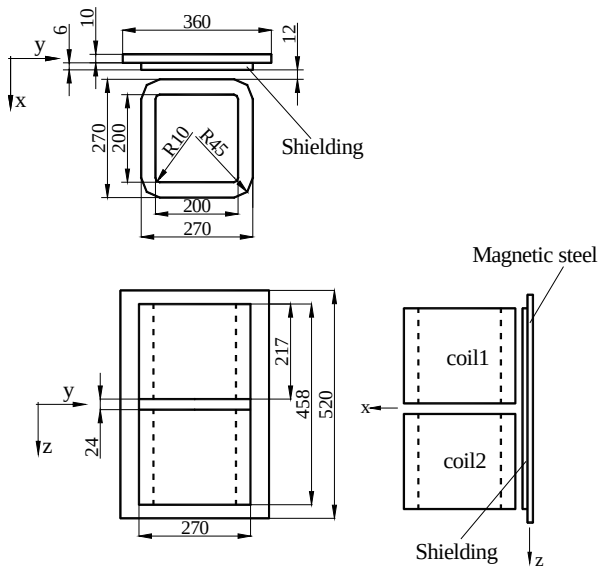

(a) P21^c-EM1 & M1

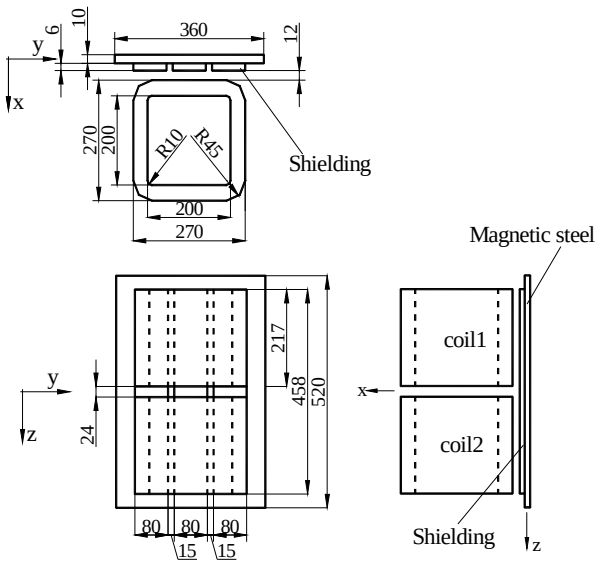

(b) P21^c-EM2 & M2

Fig. A1-4. Problem 21^c-EM & M.

==========

Appendix 2 Input and Output Data

==========

I. Input Data

There are two parts to the input data of the Problem 21 family: one is the input data for the exciting coils (referred to as the ′mother source′) common to every model; the other is the input data for the different conducting parts driven by the exciting coils, such as the magnetic steel plate, the non-magnetic steel plate, the copper plate, and the grain-oriented silicon steel sheets, which are used in different sub-models.

A. Mother Source

There are two exciting coils with the same specification, in which the exciting currents flowing in the coils are in opposite direction in the Version 2005 definition.

The number of turns of each coil: 300;

The rated exciting currents: ±10A (50Hz, rms);

The dimension of the bare copper wire: 2.0×6.7mm (net sectional area: 13.04mm^2);

The conductivity of the wire: σ=5.7143×10^7 S/m;

The assumed density of the wire: 8.9×10^{3}kg/m^3.

In the extended version of the Problem 21 definition, the exciting currents are applied with different excitation patterns and cover a range from 10 A to 50 A (50Hz, rms).

B. Conducting Parts

1) Magnetic steel plate (A3, used in P21/P21^b/P21^c)

The thickness of the plate: 10mm; the conductivity: σ= 6.484×10^6 S/m; the assumed density: 7.8×10^3 kg/m^3. The B-H and W_h-B_m curves for the isotropic magnetic steel are shown in Appendix 4 and can also be found in [1,5].

2) Non-magnetic steel (20Mn23Al, used in P21^a and P21^b)

The thickness of the plate: 10mm; The conductivity: σ= 1.3889×10^6 S/m; The relative permeability: μ_r=1.

3) Specifications of EM & M shields (used in P21^c)

Problem 21^c involves Problem 21^c-EM (P21^c-EM) and Problem 21^c-M (P21^c-M), as shown in Fig.A1-4.

P21^c-EM, as an electromagnetic screen, includes two sub-models, P21^c-EM1 and P21^c-EM2. In P21^c-EM1, a rectangular copper plate is tightly fixed on the magnetic plate of P21-B (Model B of TEAM Problem 21)[1,5], which is between the exciting coil and the magnetic plate. At the same time, P21^c-EM2 has three-pieces of parallel narrow copper plates fixed on the magnetic plate.

P21^c-M, as a magnetic shunt, also has two sub-models, 21^c-M1 and 21^c-M2. In P21^c-M1, one silicon steel lamination is fixed on the magnetic plate, while P21^c-M2 includes three sets of narrow silicon steel sheets.

3.1) Problem 21^c-EM

In P21^c-EM1, a copper plate of 458×270×6 mm is installed, but P21^c-EM2 uses three copper plates of 458×80×6 mm each. See Table A2-1. The properties of the copper plates are as follows:

The conductivity: $\sigma=5.7143\times10^7$ S/m;

The relative permeability: 1;

The assumed density: 8.9×10^3kg/m^3.

The P21^c-EM model is also shown in Fig.A1-4.

TABLE A2-1
COPPER PLATES USED IN ELECTROMAGNETIC SHIELDING MODELS

Model	Dimension (mm)	Amount	Manufacturing
P21^c-EM1	458×270×6	1	Machine cut and temper rolling
P21^c-EM2	458×80×6	3	

3.2) Problem 21^c-M

Both the size and the configuration of the P21^c-M models are the same as those of the P21^c-EM models. See Fig.A1-4. The detailed dimensions and features of the anisotropic lamination sheet used in P21^c-M are as follows:

Type of the silicon steel sheet: 30RGH120;

The length and thickness of the sheet are 458mm and 0.3mm respectively;

The width of the sheet is 270mm and 80mm for P21^c-M1 and P21^c-M2 respectively;

The Conductivity: $\sigma=2.22\times10^6$ S/m;

The assumed density: 7.65×10^3kg/m^3;

The number of silicon steel sheets laminations, for both P21^c-M1 and P21^c-M2, is equal to 20. See Table A2-2.

The B-H, W_h-B_m and W-B_m curves in both the rolling and transverse directions are listed in Appendix 4. The W_h-B_m curve indicates the hysteresis loss as a function of the peak value of the flux density, B_m. The W-B_m curve represents the relationship between the total loss (including eddy current, hysteresis and other loss component generated in silicon steel) and the peak value of the flux density, B_m.

The B-H, W_h-B_m and W-B_m curves in both the rolling direction (z-axis, see Fig.A1-4) and transverse direction (y-axis, see Fig.A1-4) of the silicon steel sheets have been measured by EPLAB of Okayama University, Japan.

Notice that Appendix 5 is helpful as a quick reference of the Problem data to be used. Appendix 6 shows the photos of all member models of Problem 21 Family.

TABLE A2-2
SILICON SHEETS USED IN MAGNETIC SHIELDING MODELS

Model	Dimension (mm)	Amount	Manufacturing
P21^c-M1	458×270×0.3	20	Machine cut
P21^c-M2	458×80×0.3	60	

II. OUTPUT DATA

A. Magnetic Flux Densities at Specified Positions

The magnetic flux densities at the specified positions, i.e. at the points where the magnetic flux enters the conducting part, and/or the points where the magnetic flux leaves the plate, should be calculated. See Table A2-3.

TABLE A2-3
RESULTS OF CALCULATED BX

z (mm)	Side where flux enters x=5+δ(or 11+δ) (mm)		Side where flux leaves x=-5-δ (mm)	
Z1				
Z2				
Z3				
.				
.				

Note: In Table A2-3, δ(herein δ=0.76mm) is the 1/2 thickness of the probe being used. The specified points on the side where the flux enters x=11+δ(mm) is for shielding model, while x=5+δ(mm) is for other models.

B. Power Loss Generated in Conducting Materials

The power loss generated in all conducting parts, such as loss in magnetic steel plate, loss in non-magnetic steel plate, loss in shielding parts (including copper plates and silicon steel lamination), should be calculated. See Table A2-4.

TABLE A2-4
RESULTS OF CALCULATED LOSS

Conducting parts	Power loss (W)			
	Eddy	Hysteresis	Excess (if necessary)	Total
Magnetic steel plate				
Non-magnetic steel plate				
Shielding parts				

Notice that it is of benefit to show the distribution of the eddy currents in the models.

==========

Appendix 3 Measured and Calculated Results at Rated Exciting Currents

==========

A number of measured and calculated results of both magnetic field and loss concerning the TEAM-based models have been obtained [1-5,7-29] at the rated exciting current of 10 A(rms, 50Hz), using $\boldsymbol{A_r}$-V-$\boldsymbol{A_r}$ –based eddy current code developed by the authors. Some of the results are shown in Table A3-1~Table A3-4 for reference.

A. Results of Magnetic Flux Density

1) Problem 21

The measured results of Bx at the specified points (x=5.76mm, y=0.0mm) for TEAM Problem 21(Model A and Model B) are listed in Table A3-1.

TABLE A3-1
MEASURED BX FOR PROBLEM 21
(PRESENTED AT TEAM-MIAMI, USA, IN 1993,)

Z(mm)	Model A	Z(mm)	Model B
	Measured ($\times 10^{-4}$T)		Measured ($\times 10^{-4}$T)
218.0	102.50	227.5	122.47
197.0	68.20	196.0	70.56
176.0	41.20	162.5	24.18
136.0	7.41	130.0	8.96
96.0	51.80	97.5	45.82
75.0	82.60	65.0	93.62
54.0	118.70	32.5	156.70
0.0	127.60	0.0	215.67
-54.0	109.90	-32.5	(1/4 symmetric)
-75.0	69.70	-65.0	____
-96.0	39.30	-97.5	____
-136.0	1.21	-130.0	____
-176.0	49.60	-162.5	____
-197.0	77.90	-196.0	____
-218.0	113.80	-227.5	____

2) Problem 21[a]

The measured and calculated (by using $\boldsymbol{A_r}$-V-$\boldsymbol{A_r}$-based program) results of Bx at the specified points (x=±5.76mm, y=0.0mm) for TEAM Problem 21[a]-2 are listed in Table A3-2.

TABLE A3-2
RESULTS OF BX FOR PROBLEM 21[a]-2
(PRESENTED AT TEAM-YICHANG, CHINA, IN 1993)

Z(mm)	X=5.76mm		x= -5.76mm	
	Measured ($\times 10^{-4}$T)	Calculated ($\times 10^{-4}$T)	Measured ($\times 10^{-4}$T)	Calculated ($\times 10^{-4}$T)
6.0	81.25	81.70	64.60	65.60
30.0	63.80	63.10	53.40	54.28
66.0	34.70	37.50	31.60	34.63
102.0	16.20	20.20	14.90	17.79
139.0	1.00	1.96	1.30	0.43
175.0	-15.50	-15.04	-12.50	-13.02
211.0	-35.10	-30.73	-27.50	-25.25
230.0	-42.00	-41.72	-32.20	-31.66
246.0	-37.20	-36.87	-29.90	-29.53
280.0	-23.70	-24.26	-20.70	-21.90
313.0	-15.30	-15.10	-13.60	-14.36
344.0	-11.20	-10.18	-9.40	-9.80
372.0	-8.70	-7.17	-6.80	-7.07
398.0	-7.60	-5.27	-5.20	-5.25

3) Problem 21[b]

The measured and calculated results of the magnetic flux density of P21[b]-MN are shown in Table A3-3.

TABLE A3-3
RESULTS OF MAGNETIC FLUX DENSITIES
(P21[b]-MN, PRESENTED AT IEE CEM, UK, 2002)

Z(mm)	x=5.76mm		X= -5.76mm	
	Measured ($\times 10^{-4}$T)	Calculated ($\times 10^{-4}$T)	Measured ($\times 10^{-4}$T)	Calculated ($\times 10^{-4}$T)
-252	-48.3	-50.3	26.3	35.5
-218	-51.0	-56.3	9.1	8.3
-197	-35.4	-36.6	7.0	7.1
-186	-25.5	-27.6	6.4	6.9
-176	-20.6	-20.1	6.0	6.6
-162	-13.4	-10.9	5.6	6.3
-136	0.0	4.13	5.1	6.2
-109	20.7	19.7	5.1	6.1
-100	26.6	25.2	5.8	6.5
-89	34.9	32.7	6.6	6.8
-75	43.8	43.3	6.8	6.7
-47	74.1	72.0	5.3	4.4
-33	91.1	91.5	-9.0	-2.0
-18	107.0	114.0	-36.1	-25.8
-9	121.0	123.0	-13.2	-4.1
-3	128.0	129.0	46.2	47.2
0	133.0	140.0	59.8	47.7
3	134.0	150.0	63.2	68.8
9	204.0	223.0	73.0	77.3
18	283.0	271.0	76.8	78.7
33	181.0	198.0	70.7	72.2
47	119.0	123.0	60.4	61.1
75	95.9	98.1	39.3	39.3
89	76.3	71.4	30.2	31.0
100	61.6	58.4	23.9	24.0
109	44.6	42.1	18.8	18.2
136	-3.58	-3.86	4.8	4.7
162	-32.4	-26.0	-8.2	-11.1
176	-46.6	-43.0	-15.6	-16.5
186	-60.4	-57.0	-21.0	-22.6
197	-75.8	-73.5	-38.4	-29.7
218	-111.0	-112.0	-41.4	-41.4
252	-146.0	-133.0	-22.8	-40.1

4) Problem 21[c]

The measured and calculated results of the magnetic flux density of P21[c]-M1(magnetic shielding model) are shown in Table A3-4.

TABLE A3-4
RESULTS OF MAGNETIC FLUX DENSITIES (P21[c]-M1)
(PRESENTED AT COMPUMAG-2005, SHENYANG)

z(mm)	x=11.76mm, y=0.0mm		x= -5.76mm, y=0.0mm	
	Measured ($\times 10^{-4}$ T)	Calculated ($\times 10^{-4}$ T)	Measured ($\times 10^{-4}$ T)	Calculated ($\times 10^{-4}$ T)
0.0	222.31	213.99	2.69	8.17
-6.0	220.31	214.00	2.68	8.15
-12.0	213.76	214.00	2.67	8.13
-18.2	201.81	187.65	2.66	6.88
-30.6	169.85	187.72	2.67	6.73
-43.0	138.95	137.19	2.69	5.62

-55.4	111.30	137.40	2.72	5.32
-67.8	89.10	93.35	2.74	4.44
-80.2	68.02	58.44	2.80	4.14
-92.6	51.05	58.90	2.88	3.64
-105.0	34.65	29.94	2.97	3.65
-117.4	20.19	30.43	3.09	3.13
-129.8	6.50	4.33	3.22	3.30
-142.2	9.20	4.72	3.42	2.84
-154.6	-22.17	-21.19	3.67	3.10
-167.0	-37.83	-50.04	4.02	3.13
-179.4	-55.86	-50.39	4.44	3.14
-191.8	-75.09	-82.263	5.07	3.27
-204.2	-98.64	-83.17	5.94	3.67
-216.6	-130.04	-143.74	7.27	4.83
-229.0	-178.97	-145.31	9.62	5.52
-241.4	-95.32	-86.86	14.12	11.10
-253.8	-100.20	-96.06	28.57	37.88
-258.0	-96.38	-95.96	45.61	38.14

B. Results of Power Loss

The measured and calculated loss results for all of TEAM-based models are shown in Table A3-5.

TABLE A3-5
MEASURED AND CALCULATED LOSS RESULTS FOR PROBLEM 21 FAMILY

Models	Measured loss (W)	Calculated loss (W)			
		Total	Losses in magnetic and/or non-magnetic steel plates		Loss in shields
			Eddy current	Hysteresis	
P21-A	9.28	9.11	6.87	2.24	
P21-B	11.97	12.04	8.10	3.94	
P21[a]-0	9.17	9.31	9.31	----	
P21[a]-1	3.40	3.34	3.34	----	
P21[a]-2	1.68	1.66	1.66	----	
P21[a]-3	1.25	1.14	1.14	----	
P21[b]–MN	7.03	6.83	5.30	1.53	
P21[b]-2M	9.34	9.88	7.44	2.44	
P21[b]-2N	1.38	1.37	1.37	----	
P21[b]–MNM	10.53	10.04	8.96	1.08	
P21[b]–NMN	7.44	7.88	6.84	1.04	
P21[c]–M1	3.72	3.79	0.90	0.30	2.59
P21[c]–M2	2.64	3.16	1.65	0.68	0.83
P21[c]–EM1	15.24	16.22	3.87	1.50	10.85
P21[c]–EM2	20.07	20.11	8.45	2.35	9.31

==========

Appendix 4 Property Data of Magnetic Steel

==========

A. Magnetic Steel (A3)

The B-H curve and W_h-B_m curve of the magnetic steel plates (A3) used in Problem 21 Family were measured in EPLAB, Okayama University, Japan, as shown in Table A4-1. The conductivity of the plate is 6.484×10^6 S/m.

TABLE A4-1
B-H CURVE AND W_h-B_m CURVE OF MAGNETIC STEEL (A3)

B(T)	H (A/m)	W_h (W/kg)	B(T)	H (A/m)	W_h (W/kg)
0.049	115	0.02	1.449	1965	11.86
0.101	171	0.11	1.500	2506	12.80
0.150	196	0.24	1.550	3291	13.77
0.200	214	0.41	1.600	4430	14.68
0.299	245	0.82	1.639	5599	15.28
0.399	279	1.32	1.670	6698	15.73
0.499	316	1.88	1.701	7926	16.22
0.601	359	2.51	1.729	9251	16.84
0.700	405	3.21	1.760	10792	17.32
0.801	461	3.98	1.781	11930	17.51
0.899	528	4.82	1.800	13106	17.57
1.001	616	5.77	1.830	14949	17.75
1.099	732	6.81	1.850	16290	17.72
1.200	898	8.01	1.875	18002	17.82
1.300	1154	9.39	1.900	19942	17.85
1.401	1606	10.99			

B. Grain-Oriented Silicon Steel Sheet

The B_m-H_b, W_h-B_m and W-B_m curves of the anisotropic silicon steel sheet (30RGH120) used in P21[c] and P21[d]-M were measured in EPLAB, Okayama University, Japan, as shown in Tables A4-2~A4-6 and Figs.A4-1~A4-6.

TABLE A4-2
B-H CURVE OF SILICON STEEL IN ROLLING DIRECTION (30RGH120)

B_m[T]	H_b[A/m]	B_m[T]	H_b[A/m]
0.0500	1.5757	1.0496	9.6248
0.1000	2.5912	1.0998	9.8313
0.1501	3.4846	1.1497	10.2613
0.2001	4.2920	1.1998	10.6696
0.2501	4.9280	1.2497	11.2566
0.3001	5.5596	1.2997	12.0681
0.3501	6.0624	1.3496	13.1694
0.4002	6.3726	1.3997	15.0969
0.4502	6.8566	1.4496	17.6901
0.5001	7.0721	1.4997	21.2103
0.5503	7.4201	1.5494	26.2651
0.6000	7.6989	1.5994	33.4483
0.6503	7.8836	1.6495	46.9983
0.7004	8.1211	1.6995	69.1130
0.7504	8.3246	1.7494	105.8169
0.8004	8.6006	1.7994	182.9606
0.8504	8.7677	1.8491	357.9689
0.9004	8.9253	1.8991	742.4458
0.9497	9.1544	1.9490	1667.8985
1.0001	9.3758	1.9990	9081.6648

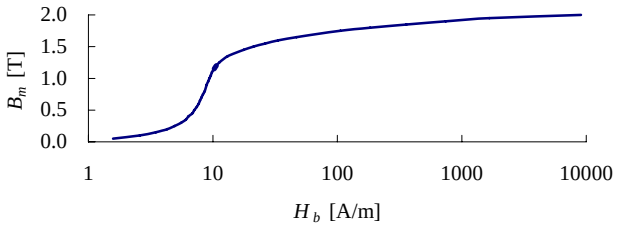

Fig. A4-1. B-H curve of silicon steel (in rolling direction, 30RGH120).

TABLE A4-3
B-H CURVE OF SILICON STEEL IN
TRANSVERSE DIRECTION (30RGH120)

B_m [T]	H_b [A/m]	B_m [T]	H_b [A/m]
0.0501	85.3664	1.0489	189.4970
0.1000	120.8005	1.0999	196.7729
0.1493	135.6965	1.1490	208.2999
0.2006	144.5633	1.1998	232.3968
0.2489	150.0459	1.2492	289.9317
0.3002	154.0995	1.2997	433.3158
0.3494	157.5049	1.3491	736.1902
0.4004	159.7633	1.3997	1366.9074
0.4494	161.6266	1.4492	2361.8001
0.5001	163.9006	1.4996	3698.2184
0.5493	165.3869	1.5491	5293.3038
0.6004	166.8455	1.5993	7186.9947
0.6492	168.3099	1.6493	9316.4081
0.7000	169.6325	1.6990	11650.1128
0.7491	171.4374	1.7492	14193.6353
0.8002	173.1495	1.8001	16952.0366
0.8492	175.3864	1.8501	19834.8760
0.8999	178.1123	1.9001	22893.7254
0.9490	181.0530	1.9502	26145.8958
0.9998	184.8982	2.0002	29665.5458

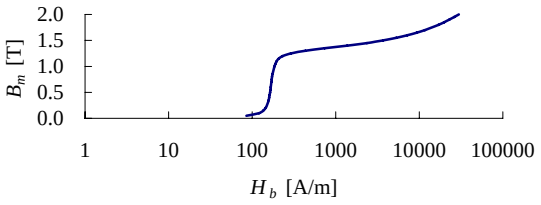

Fig. A4-2. B-H curve of silicon steel (in transverse direction, 30RGH120).

Note that H_b in Table A4-2 and Table A4-3 is the value of the magnetic field intensity H when the flux density becomes the maximum (B_m). The reason for using the value at B_m and H_b is that the eddy current becomes almost zero at this instant. This means that the measured B_m-H_b curve is nearly dc B-H curve.

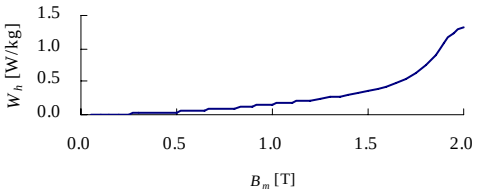

Fig.A4-3. W_h-B_m curve of silicon steel (in rolling direction, 50Hz, 30RGH120).

TABLE A4-4
W_h-B_m CURVE OF SILICON STEEL IN
ROLLING DIRECTION (50HZ, 30RGH120)

B_m[T]	W_h[W/kg]	B_m[T]	W_h [W/kg]
0.0500	0.0007	1.0498	0.1693
0.1000	0.0022	1.0998	0.1839
0.1501	0.0046	1.1498	0.2028
0.2001	0.0077	1.1997	0.2224
0.25011	0.0122	1.2495	0.2431
0.3002	0.0166	1.2996	0.2588
0.3501	0.0222	1.3493	0.2793
0.4001	0.0284	1.3995	0.3035
0.4502	0.0370	1.4495	0.3313
0.5002	0.0435	1.4995	0.3536
0.5502	0.0521	1.5489	0.3885
0.6002	0.0610	1.5988	0.4280
0.6502	0.0726	1.6485	0.4811
0.7003	0.0800	1.6989	0.5439
0.7501	0.0918	1.7492	0.6348
0.8002	0.1022	1.7992	0.7610
0.8501	0.1165	1.8493	0.9071
0.9001	0.1279	1.8993	1.0725
0.9500	0.1434	1.9491	1.2449
1.0000	0.1561	1.9992	1.3170

TABLE A4-5
W_h-B_m CURVE OF SILICON STEEL IN
TRANSVERSE DIRECTION (50HZ, 30RGH120)

B_m [T]	W_h [W/kg]	B_m [T]	W_h [W/kg]
0.0501	0.0204	0.8498	0.9289
0.1003	0.0648	0.8999	0.9896
0.1500	0.1187	0.9496	1.0490
0.2001	0.1774	0.9997	1.1130
0.2499	0.2369	1.0495	1.1784
0.3001	0.2993	1.0995	1.2481
0.3499	0.3589	1.1494	1.3293
0.4002	0.4191	1.1994	1.4254
0.4500	0.4771	1.2494	1.5539
0.4999	0.5358	1.2996	1.7322
0.5499	0.5932	1.3493	1.9579
0.6000	0.6502	1.3994	2.2127
0.6499	0.7058	1.4494	2.4482
0.6999	0.7613	1.4993	2.6532
0.7499	0.8164	1.5492	2.8002
0.7999	0.8725	1.5993	2.9182

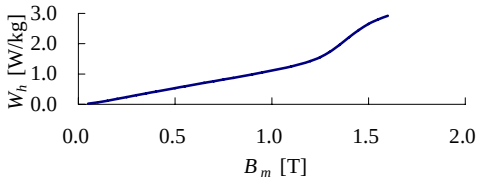

Fig. A4-4. W_h-B_m curve of silicon steel (in transverse direction, 50Hz, 30RGH120).

TABLE A4-6
W-B_m CURVE OF SILICON STEEL (50HZ, 30RGH120)

In Rolling direction		In transverse direction	
B_m [T]	W [W/kg]	B_m [T]	W [W/kg]
0.0500	0.0011	0.0500	0.0290
0.1000	0.0040	0.1000	0.0922
0.1501	0.0088	0.1493	0.1685
0.2001	0.0151	0.2006	0.2526
0.2501	0.0226	0.2489	0.3344
0.3001	0.0324	0.3002	0.4224
0.3501	0.0436	0.3494	0.5048
0.4002	0.0549	0.4004	0.5910
0.4502	0.0704	0.4494	0.6719
0.5001	0.0850	0.5001	0.7566
0.5503	0.1012	0.5493	0.8374
0.6000	0.1202	0.6004	0.9218
0.6503	0.1426	0.6492	0.9994
0.7004	0.1626	0.7001	1.0838
0.7504	0.1886	0.7491	1.1651
0.8004	0.2090	0.8002	1.2501
0.8504	0.2352	0.8492	1.3342
0.9004	0.2580	0.8999	1.4246
0.9497	0.2946	0.9490	1.5123
1.0001	0.3213	0.9998	1.6041
1.0496	0.3557	1.0489	1.6978
1.0998	0.3861	1.0999	1.8012
1.1497	0.4234	1.1490	1.9122
1.1998	0.4503	1.1998	2.0386
1.2497	0.4977	1.2492	2.1965
1.2997	0.5355	1.2997	2.4087
1.3496	0.5806	1.3491	2.6844
1.3997	0.6227	1.3996	2.9984
1.4496	0.6770	1.4492	3.2752
1.4997	0.7234	1.4996	3.5174
1.5494	0.7834	1.5491	3.6992
1.5994	0.8487	1.5993	3.8528
1.6495	0.9241	1.6493	3.9627
1.6995	1.0100	1.6990	4.0424
1.7494	1.1262	1.7492	4.0971
1.7994	1.2803	1.8001	4.1714
1.8491	1.4580	1.8501	4.2433
1.8991	1.6727	1.9001	4.3202
1.9490	1.9030	1.9502	4.4122
1.9990	2.1173	2.0002	4.5229

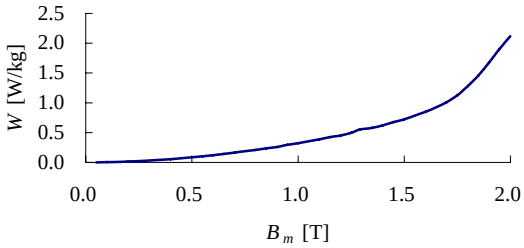

Fig. A4-5. W-B_m curve of silicon steel (in rolling direction, 50Hz, 30RGH120).

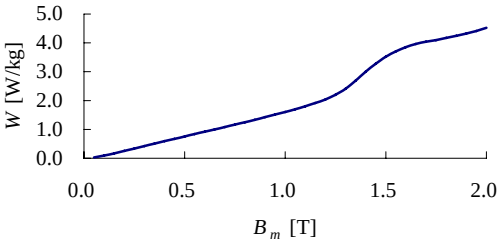

Fig. A4-6. W-B_m curve of silicon steel (in transverse direction, 50Hz, 30RGH120).

Note that in Fig.A4-5~Fig.A4-6 and Table A4-6 'W' stands for the total loss per kilogram of silicon steel sheet.

==========

Appendix 5 Reference Data

==========

Some input data of Problem 21 Family are re-listed in Table A5-1 ~A5-2 for quick reference.

TABLE A5-1
DIMENSION OF CONDUCTING PARTS

Model	Magnetic steel plate (A3)		Non-magnetic steel plate (20Mn23Al)		Silicon steel sheet (30RGH120)		Copper plate	
	Size (mm)	Number	Size (mm)	Number	Size (mm)	Number	Size (mm)	Number
P21-A	360×248×10	2						
P21-B	360×520×10	1						
P21[a]-0			360×820×10	1				
P21[a]-1			360×820×10	1				
P21[a]-2			360×820×10	1				
P21[a]-3			360×820×10	1				
P21[b]-MN	360×248×10	1	360×248×10	1				
P21[b]-2M	360×248×10	2						
P21[b]-2N			360×248×10	2				
P21[c]-M1	360×520×10	1			270×458×0.3	20		
P21[c]-M2	360×520×10	1			80×458×0.3	20×3		
P21[c]-EM1	360×520×10	1					270×458×6	1
P21[c]-EM2	360×520×10	1					80×458×6	3
P21[d]-M					270×458×0.3	20		

TABLE A5-2
PERFORMANCE DATA OF CONDUCTING PARTS

Performance	Magnetic steel plate (A3)	Non-magnetic steel plate (20Mn23Al)	Silicon steel sheet (30RGH120)	Copper plate
Conductivity (S/m)	6.484×10^{6}	1.3889×10^{6}	2.22×10^{6}	5.7143×10^{7}
Assumed density (kg/m^3)	7.80×10^{3}	7.80×10^{3}	7.65×10^{3}	8.90×10^{3}
B-H curve (isotropic)	Appendix 4 (Table A1)			
W_h-B_m curve (isotropic)	Appendix 4 (Table A4-1)			
B-H curve in rolling direction (z-axis)			Appendix 4 (Table A4-2)	
B-H curve in transverse direction (y-axis)			Appendix 4 (Table A4-3)	
W_h-B_m curve in rolling direction (z-axis)			Appendix 4 (Table A4-4)	
W_h-B_m curve in transverse direction (y-axis)			Appendix 4 (Table A4-5)	
W-B_m in rolling direction (z-axis)			Appendix 4 (Table A4-6)	
W-B_m curve in transverse direction (y-axis)			Appendix 4 (Table A4-6)	

==========

Appendix 6 Problem 21 Family (1993-2009)

==========

A benchmark family including 16 models has been established, see Figs.A6-1~A6-5.

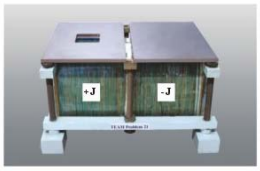

Model A Model B

Fig. A6-1. Principal models (1993: 3-D eddy current/hysteresis model with multiply connected magnetic steel plates).

P21[a]-0 P21[a]-1 P21[a]-2 P21[a]-3

Fig. A6-2. P21[a] (1996: 3-D linear eddy current model with multiply connected non-magnetic steel plate).

P21[b]-MN P21[b]-2N P21[b]-2M (2002)

P21[b]-NMN P21[b]-MNM (2006)

Fig. A6-3. P21[b] (2002, 2006: 3-D nonlinear eddy current/hysteresis model with magnetic (M) and/or non-magnetic (N) steel plates, which are separately placed or welded together).

P21[c]-M1 P21[c]-M2 P21[c]-EM1 P21[c]-EM2

Fig. A6-4. P21[c] (2005: 3-D magnetic shielding (P21[c]-M1/M2 with lamination) and electromagnetic shielding(P21[c]-EM1/EM2 with copper plate) models, in which magnetic plate is shielded).

P21[d]-M

Fig. A6-5. P21[d]-M (2008: 3-D nonlinear eddy current/hysteresis model with anisotropic lamination without solid magnetic plate).